J Computer-Aided Mater Des
DOI 10.1007/s10820-006-9040-y

Discrete size series of CdSe quantum dots: a combined computational and experimental investigation

M. Yu · G. W. Fernando · R. Li · F. Papadimitrakopoulos · N. Shi · R. Ramprasad

Received: 3 June 2006 / Accepted: 1 September 2006

Abstract Ab initio computational studies were performed for CdSe nanocrystals (NCs) over a wide variety of sizes ranging from 8 to 150 atoms in conjunction with recent experimental work. The density functional based calculations indicate substantial relaxations. Changes in coordination of surface atoms were found to play a crucial role in determining the NC stability and optical properties. While optimally (threefold) coordinated surface atoms resulted in stable closed-shell structures with large optical gaps, sub-optimal coordination gave rise to lower stability and negligible optical gaps. These computations are in qualitative agreement with recent chemical etching experiments suggesting that closed shell NCs contribute strongly to photoluminescence quantum yield while clusters with nonoptimal surface coordination do not.

Keywords Semiconductor quantum dots · Cadmium compounds · Ab initio calculation · Energy gap · Photoluminescence · Surface structure

1 Introduction

The size, shape, and surface passivation of semiconductor CdSe nanocrystals (NCs) have been a topic of intense theoretical and experimental investigations, in light of their effect on their optical and electronic properties [1,2]. Their tunable emission,

M. Yu · G. W. Fernando
Department of Physics, University of Connecticut, Storrs, CT 06269, USA

R. Li · F. Papadimitrakopoulos
Polymer Program and Department of Chemistry, University of Connecticut, Storrs, CT 06269, USA

N. Shi · R. Ramprasad (✉)
Department of Chemical, Materials and Biomolecular Engineering, University of Connecticut, Storrs, CT 06269, USA
e-mail: rampi@uconn.edu

enhanced photo-oxidation stability, and electron transporting nature render them ideal candidates for applications on biological labels [3,4], laser media [5], light emitting diodes [1,2], nonlinear optics [6,7], and photovoltaics [8]. Although considerable understanding has been achieved in terms of quantum confinement, much less is known about the state of bonding and disorder at NC surfaces [1,2]. The size discrepancy between effective sizes obtained from small angle X-ray diffraction and transmission electron microscopic (TEM) results [9] has been attributed to the lack of order of the outermost surface layer. This layer, together with the variety of passivating agents is deemed essential for cladding these NCs to achieve high-photoluminescence (PL) efficiency (i.e., as high as 50%) [10]. If however, various asperities (such as vacancies, incomplete coverage, and dangling bonds) are present at the outermost surface layer, NC PL efficiency is severely reduced [1,2].

2 Modeling and computational details

This study intends to provide a more comprehensive understanding of the influence of surface imperfections on the electronic properties of CdSe NCs. In particular, first principles computational methods have been employed to determine local structure at the NC surface in relation to their contribution to the NC density of states (DOS), which ultimately control optical properties. CdSe NCs with diameters up to 2 nm (150 atoms, or 75 CdSe pairs) were investigated as a function of number of CdSe pairs to emulate close- and open-shelled structures. Our findings are in qualitative agreement with respect to the experimental results obtained for PL efficiency as a function of NC size [11–13]. These combined computational-experimental studies reveal cyclic modulation of PL quantum efficiencies with respect to the average NC diameter.

Prior computational studies of CdSe clusters fall in two broad classes: (1) efforts based on classical molecular dynamics, and first principles techniques without self-consistency or geometry optimization, involving a wide range of cluster sizes [14–18], and (2) sophisticated self-consistent ab initio calculations that treat only small or limited cluster sizes [19–21]. Owing to an inadequate treatment of the electronic/structural degrees of freedom, the former type of calculations may lead to erroneous conclusions concerning the impact of surface relaxations on optical properties, as pointed out recently [19]. For example, a recent classical molecular dynamics study [15] suggested that Cd and Se atoms in successive layers tend to attract one another leading to a "pinching" effect. This effect, not seen in our work, is most likely due to overestimation of the Coulomb interactions resulting from potentials that do not respond to relaxations in electronic structure. We are also aware of a recent tight-binding calculation [18] where the surface Cd atoms were left unrelaxed. Our calculations show that the surface Cd atoms prefer to move inwards. The second class of calculations referred to above provide very accurate information concerning the stability, structure, and optical properties of small semiconductor clusters [19–21]. However, to the best of our knowledge, we are not aware of a systematic study of trends in such properties over a wide range of experimentally relevant cluster sizes at a high level of theory. We believe that our study fills this void while maintaining a close connection with parallel experimental work.

All calculations reported here were performed using the local density approximation (LDA) within DFT [22] as implemented in the local orbital SIESTA code [23]. Norm-conserving nonlocal pseudopotentials of the Troullier–Martins type [24] were

used to describe all the elements, with Cd and Se at the $[\mathrm{Kr}]5s^2 4d^{10}$ and $[\mathrm{Ar}3d^{10}]4s^2 4p^4$ atomic configurations, respectively. A double-zeta plus polarization (DZP) basis set was used for all calculations. The equilibrium positions of the atoms were determined by requiring the forces on each atom to be smaller than $0.04\,eV/\text{Å}$.

3 Computational results

As a test of the pseudopotentials and computational method, bulk CdSe calculations in the zinc blende and wurtzite phases were performed. The calculated lattice constant for the zinc blende phase was 6.15 Å, and those for the wurtzite phase were 4.31 and 6.84 Å. These calculated values compare well with the experimental values [25,26] of 6.05 Å for zinc blende and 4.30 and 7.01 Å for the wurtzite phase. Thus, the structural parameters for the bulk crystalline materials were well reproduced.

Stoichiometric CdSe clusters based on an underlying wurtzite crystal structure with an approximately spherical shape were considered in all calculations. The wurtzite structure is the hexagonal analogue of the (cubic) zinc blende structure, and has hexagonal $\cdots ABAB \cdots$ packing, with a two-atom basis. In CdSe, a Cd and a Se atom form the basis and one of their (nearest neighbor) bonds is directed along the *c*-axis, perpendicular to A or B planes, as can be seen in the unit cell shown in Fig. 1 (middle, bottom). Spherical clusters, based on the wurtzite structure, could be generated using one of several choices for the cluster center or origin. The choice of the center and the radius will determine the (chemical) type of the atoms that occupy the surface region. In this work, we have considered three choices of the center, O1, O2, and O3, shown in the unit cell of Fig. 1 as follows: (1) the midpoint of a nearest neighbor Cd–Se bond along the $\hat{a}_3$ direction, i.e., O1 $\equiv (0, 0, u/2)$, (2) the point at a distance $c/2$ from O1 along the $\hat{a}_3$ direction, i.e., O2 $\equiv (0, 0, (c+u)/2)$, and (3) O3 $\equiv (a/3, a/3, u/2)$. Here $u(= 0.37c)$ denotes the nearest neighbor Cd–Se distance (i.e., Cd–Se bond length) in bulk wurtzite CdSe, while a and c are the lattice parameters in the standard notation. The coordinates are given with respect to axes that define the unit cell indicated in Fig. 1. Our choice of wurtzite being the underlying crystal structure of all CdSe clusters studied computationally was guided by High Resolution Transmission Electron Microscopy (HRTEM) measurements of synthesized CdSe NCs, a micrograph of which is also shown in Fig. 1 (middle, top).

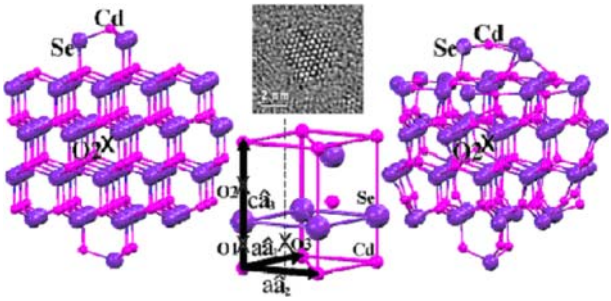

Fig. 1 The 144 atom CdSe nanocluster (with center O2) before (*left*) and after (*right*) geometry optimization. An HRTEM image (*middle, top*) and a CdSe wurtzite crystal unit cell (*middle, bottom*) with connectivity between atoms chosen to clarify the location of origins are also shown

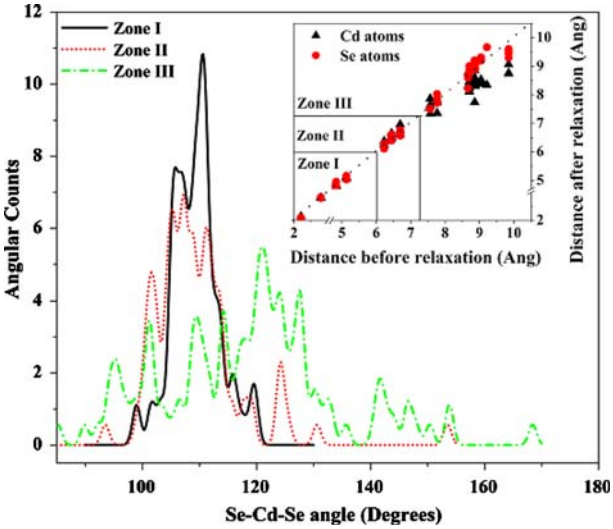

Fig. 2 Angular and radial (inset) relaxations for the 144 atom CdSe cluster. Points that fall on the *dotted line* in the inset correspond to atoms that have not relaxed radially

For each of the three choices of the center of the clusters, a wide variety of sizes ranging from 8 to 150 atoms were considered. The electronic and geometric structures were optimized for all these clusters, resulting in equilibrium physical structures, total energies, DOS and HOMO–LUMO gaps, which form the basis of all our conclusions. First, we discuss the calculated structural relaxations for a particular CdSe cluster, namely, the 144 atom cluster (with center at O2), whose geometry before and after structural optimization is shown in Fig. 1. Fig. 2 (inset) shows the calculated (radial) structural relaxations of this cluster from its initial starting geometry [which was based on an ideal wurtzite structure, Fig. 1 (left)]. The dotted line represents the situation with no radial relaxations. For clarity, we have divided the regions occupied by the atoms of the NC into three mutually exclusive zones. In Zone I, extending from the origin to 6 Å, atoms undergo negligible radial relaxations; this zone is thus the "core region" which is well screened from the surface atoms. In Zone II, Cd and Se atoms show small but perceptible relaxations. In Zone III, which consists mainly of surface atoms, Cd atoms prefer to move radially inward while some Se atoms move radially outward. This inward relaxation of Cd atoms has been observed in other self-consistent calculations [19].

Fig. 2 also shows the angular distribution of Se–Cd–Se bond angles of the same 144 atom cluster. In the core region (Zone I), most of the Se–Cd–Se angles are within a few percent of the tetrahedral (109.5°) angle, indicating predominantly sp^3 bonding. The corresponding angles in Zones II and III show progressively more dispersion, indicating that sp^3 like bonds between Cd and its four neighboring Se atoms are not the dominant ones (especially in Zone III, where angles in the neighborhood 120° dominate, characteristic of sp^2 bonding).

The total energies and HOMO–LUMO gaps calculated for clusters up to 75 CdSe pairs (150 atoms) are shown in Fig. 3 (inset). Several interesting trends can be observed. First, the total energy per CdSe pair, Etotal/Pair, converges steadily with increasing cluster size. However, Etotal/Pair shows local minima, reminiscent of the so-called "magic sizes" [27–29], with clusters composed of 13, 17, 26, 35, 48, 69, and

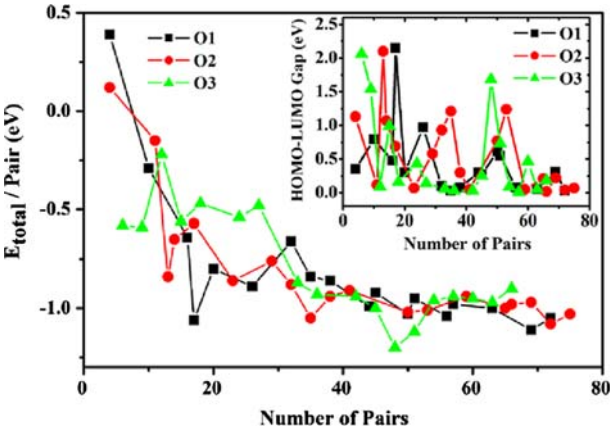

Fig. 3 Calculated total energies per pair of the fully relaxed CdSe nanoclusters and the HOMO–LUMO gaps (inset) as a function of the nanocluster size (number of CdSe pairs) for three different choices, O1, O2, O3, of origin. Note the correlation between high stability and large HOMO–LUMO gaps, especially for smaller clusters containing 60 or less pairs

72 pairs displaying the maximum relative stability. Second, the stability is strongly a function of the choice of origins, especially for the small clusters. Third, while the HOMO–LUMO (or optical) gaps generally decrease for increasing cluster sizes, occasional large gaps can be seen that correlate with a low Etotal/Pair (or high stability); i.e., the "magic size" clusters show relatively large, and locally largest, gaps.

Inspection of the physical structure of the clusters indicates that the nonmagic size clusters have surface atoms with a high degree of unsaturation (two or more dangling bonds). These surface atoms give rise to electronic states resulting in an apparent reduction in the HOMO–LUMO gap. This expectation is confirmed by explicit analysis of the DOS, and its decomposition in terms of the contributions from various atomic basis functions (the partial density of states, or PDOS). Fig. 4a, for instance, shows a large HOMO–LUMO gap in a DOS plot for the 17-pair magic cluster with origin at O1. For such a cluster, all surface atoms have three bonds with their nearest neighbor atoms. On the other hand, by changing the origin to O2, a similar 17-pair cluster has 4 Cd and 4 Se surface atoms bonded to only two as opposed to three nearest neighbor atoms. This results in a much smaller HOMO–LUMO gap as shown in Fig. 4b. Analysis of the PDOS for the 17-pair cluster with center at O2 in fact demonstrates that the origin of the smaller gap is due to states created by the surface atoms with missing or dangling bonds. Upon closer inspection of all simulated clusters, those which have surface atoms missing one or more bonds show uniformly smaller nonwell defined gaps.

4 Experimental results

The current results shed considerable light on a number of experimental studies alleging optimum performance on CdSe NCs with closed-shell structures [11–13]. In our experiment, the APOL-capped CdSe NCs were etched in the APOL/H2O (v/v = 10:1) annealing solution at 85 ± 5° C. The change in PL peak position, quantum yield (QY),

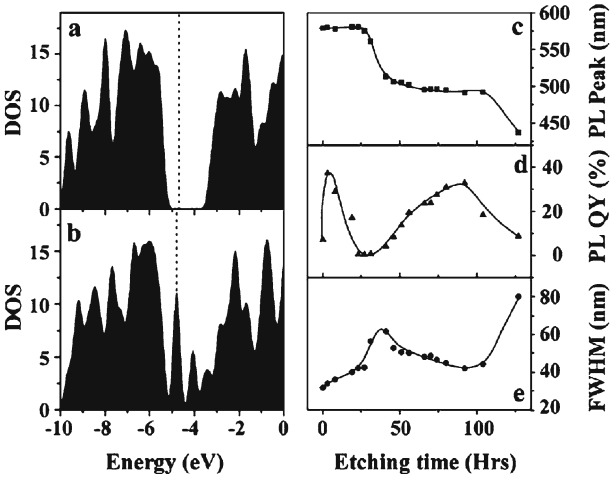

Fig. 4 Calculated density of states (*DOS*) for a nanocluster with 17 CdSe pairs, with center at **a** O1 and at **b** O2. The Fermi level is indicated by the *vertical dotted lines*. **c** Measured photoluminescence (*PL*) peak positions, **d** quantum yield (*QY*), and **e** PL full-width-at-half-maximum, as a function of nanocluster etching time. The plateaus that develop with etching time in **c** indicate the relative stability of nanoparticles with closed shell structures

and full-width-at-half-maximum (FWHM) of the annealed CdSe NCs were observed. The evolution of the UV/Vis absorption and PL emission of CdSe NCs as a function of annealing time were also observed.

Fig. 4c, d, e shows the PL peak position, QY or efficiency, and the PL FWHM as a function of etching time, which is inversely related to their size (from diameter of 3.4 nm at the beginning to 2.2 nm after 80 h). Each well defined step (plateau region) in PL peak position corresponds to a Cd-terminated closed-shell NC with a specific size [11,12]. Such discrete PL emission along with the peaking of QY in the plateau regions can be explained in terms of: (1) more NCs attain closed-shell structures (during etching) that emit strongly, and (2) upon further etching, NC of nonclosed-shell structures are created that exhibit little or no luminescence thereby causing a decrease in the QY. Such nonclosed-shell NC structures are expected to contain surface atoms with less than the optimal, threefold coordinated bonding arrangement causing them to lack well defined optical gaps, as in the case of Fig. 4b. Surface atoms with lower than the optimum threefold bonding arrangement possess higher chemical reactivity, thereby explaining the relative thermodynamic stability of closed-shell structures against etching.

Furthermore, controlled chemical etching has also been used to investigate the evolution of UV-Vis [Fig. 5 (left)] and PL properties [Fig. 5 (right)] of CdSe quantum dots as a function of NC size [11,12]. The experimental results suggest that CdSe NCs of certain structures show high PL quantum yield. During the etching process, when the population of CdSe NCs with this structure (e.g., NCs with the diameter of 3.4 nm which emit at 580 nm) increases, the PL intensity increases. Upon further etching, CdSe NCs of this structure are gradually destroyed, decreasing the PL intensity. Only when the structure reaches the next stable structure of smaller size (e.g., NCs with the diameter of 2.2 nm which emit at 495 nm), the PL intensity increases again. It is interesting to notice that the size difference between these two NCs is about 1.3 nm,

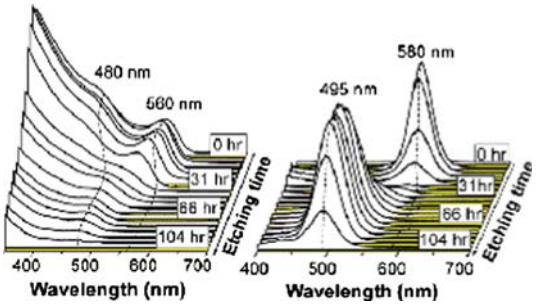

Fig. 5 (*left*) UV/Visible and (*right*) photoluminescence (*PL*) spectra for selected CdSe nanoclusters. Note the blue shift that develops with etching time in both spectroscopies. Also note the variation in the peak PL intensities as a function of etching time

almost the same size difference expected from removing one layer of CdSe from the CdSe NC surface. These observations suggest that CdSe NCs with closed shell structures show high-PL efficiency, that etching destroys this structure, and consequently, the PL intensity decreases. Only when the NC reaches the next closed shell structure by removing one layer of CdSe from the surface, the PL intensity increases again.

5 Summary

We have performed self-consistent ab initio calculations and experimental studies to understand the stability of CdSe clusters, and the relationship between cluster size and optical properties of CdSe clusters over a wide range of sizes. Our calculations indicate that the nature of the surface atoms in a given cluster crucially determines both the stability of the cluster and its optical gap. When the NCs were allowed to relax from their bulk wurtzite positions, Cd atoms at the surface are observed to move inwards preferentially compared to Se atoms. A coordination number of three for all surface atoms resulted in closed-shell structures with high stability and maximum optical gap. One or more sub-optimally coordinated surface atoms resulted in clusters with lower stability and smaller to negligible optical gaps. These computations are in qualitative agreement with recent chemical etching experiments suggesting that closed shell NC structures contribute strongly to PL quantum yield while clusters with less than optimal surface coordination do not, evident from the plateaus (in etching time) seen in PL peak positions, and the quantum efficiency peak within each PL plateau.

References

1. Murray, C.B., Kagan, C.R., Bawendi, M.G.: Annu. Rev. Mater. Sci. **30**, 545 (2000)
2. Alivisatos, A.P.: J. Phys. Chem. **100**, 13226 (1996)
3. Chan, W.CW., Maxwell, D.J., Gao, X., Bailey, R.E., Han, M., Nie, S.: Curr. Opin. Biotechnol. **13**, 40 (2002)
4. Han, M., Gao, X., Su, J.Z., Nie, S.: Nat. Biotechnol. **19**, 631 (2001)
5. Klimov, V.I., Mikhailovsky, A.A., Xu, S., Malko, A., Hollingsworth, J.A., Leatherdale, C.A., Eisler, H.J. Bawendi, M.G.: Science **290**, 314 (2000)
6. Ispasoiu, R.G., Lee, J., Papadimitrakopoulos, F., Goodson, T. III: Chem. Phys. Lett. **340**, 7 (2001)
7. Ispasoiu, R.G., Jin, Y., Lee, J., Papadimitrakopoulos, F., Goodson, T. III: Nano Lett. **2**, 127 (2002)

8. Huynh, W.U., Dittmer, J.J., Alivisatos, A.P.: Science **295**, 2425 (2002)
9. Peng, X., Wickham, J., Alivisatos, A.P.: J. Am. Chem. Soc. **120**, 5343 (1998)
10. Talapin, D.V., Rogach, A.L., Kornowski, A., Haase, M., Weller, H.: Nano. Lett. **1**, 207 (2001)
11. Li, R., Lee, J., Yang, B., Horspool, D.N., Aindow, M., Papadimitrakopoulos, F.: J. Am. Chem. Soc. **127**, 2524 (2005)
12. Li, R., Lee, J., Kang, D., Luo, Z., Aindow, M., Papadimitrakopoulos, F.: Adv. Funct. Mater. **16**, 345 (2006)
13. Talapin, D.V., Rogach, A.L., Shevchenko, E.V., Kornowski, A., Haase, M., Weller, H.: J. Am. Chem. Soc. **124**, 5782 (2002)
14. Sarkar, P., Springborg, M.: Phys. Rev. B **68**, 235409 (2003)
15. Rabani, E.: J. Chem. Phys. **115**, 1493 (2001)
16. Eichkorn, K., Alrichs, R.: Chem. Phys. Lett. **288**, 235 (1998)
17. Wang, L.W., Zunger, A.: Phys. Rev. B **53**, 9579 (1996)
18. Pokrant, S., Whaley, K.B.: Eur. Phys. J. D **6**, 255 (1999)
19. Puzder, A., Williamson, A.J., Gygi, F., Galli, G.: Phys. Rev. Lett. **92**, 217401 (2004)
20. Kasuya, A., et al.: Nature **3**, 99 (2004)
21. Troparevsky, M.C., Kronik, L., Chelikowsky, J.R.: Phys. Rev. B **65**, 033311 (2002)
22. Martin, R.: Electronic Structure: Basic Theory and Practical Methods. Cambridge University Press, New York (2004)
23. Soler, J.M., Artacho, E., Gale, J., Garcia, A., Junquera, J., Ordejon, P., Sanchez-Portal, D.: J. Phys.: Condens. Matter **14**, 2745 (2002)
24. Troullier, N., Martins, J.L.: Phys. Rev. B **43** 1993 (1991)
25. Zakharov, O., Rubio, A., Blasé, X., Cohen, M.L., Louie, S.G., Phys. Rev. B **50**, 10780 (1994)
26. Hellwege, K.-H., Madelung, O.: Numerical Data and Functional Relationships in Science and Technology, Landolt-Bornstein, New Series, Group III, vol. 17a, 22a. Springer, Berlin Heidelberg, New York (1982)
27. Brus, L.E.: J. Phys. Chem. **90**, 2555 (1986)
28. Peng, Z.A., Peng, X.: J. Am. Chem. Soc. **124**, 3343 (2002)
29. Soloviev, V.N., Eichhöfer, A., Fenske, D., Banin, U.: J. Am. Chem. Soc. **122**, 2673 (2000)